

# Time-Resolved Photoelectron Angular Distributions from Strong-Field Ionization of Rotating Naphthalene Molecules

Jonas L. Hansen<sup>1</sup> and Henrik Stapelfeldt<sup>1,2,\*</sup>

<sup>1</sup>*Interdisciplinary Nanoscience Center (iNANO), Aarhus University, 8000 Aarhus C, Denmark*

<sup>2</sup>*Department of Chemistry, Aarhus University, DK-8000 Aarhus C, Denmark*

Darko Dimitrovski,<sup>3</sup> Mahmoud Abu-samha,<sup>3</sup> Christian P.J. Martiny,<sup>3</sup> and Lars Bojer Madsen<sup>3,†</sup>

<sup>3</sup>*Lundbeck Foundation Theoretical Center for Quantum System Research, Department of Physics and Astronomy, Aarhus University, DK-8000 Aarhus C, Denmark*

(Received 1 November 2010; published 15 February 2011)

A nanosecond laser pulse confines the spatial orientation of naphthalene in 1D or 3D while a femtosecond kick pulse initiates rotation of the molecular plane around the fixed long axis. Time-dependent photoelectron angular distributions (PADs), resulting from ionization by an intense femtosecond probe pulse, exhibit pronounced changes as the molecular plane rotates. Enhanced 3D alignment, occurring shortly after the kick pulse, provides strongly improved contrast in molecular-frame PADs. Calculations in the strong-field approximation show that the striking structures observed in the PADs originate from nodal planes in occupied valence orbitals.

DOI: 10.1103/PhysRevLett.106.073001

PACS numbers: 33.80.Rv, 33.60.+q, 33.80.Eh, 42.50.Hz

Time-resolved photoelectron spectroscopy is a promising ultrafast technique for characterizing the electronic and nuclear dynamics occurring after photoabsorption in polyatomic molecules. The basic principle, employed in almost all studies to date, consists of initiating a photoinduced process in a molecule by a femtosecond (fs) pump pulse and probing the evolution of the process by detecting the kinetic energy distribution of the photoelectrons created through ionization with a delayed fs probe pulse [1,2]. Yet, there is one more experimental observable, namely, the emission direction of the electrons, i.e., the photoelectron angular distribution (PAD) [3]. It provides additional information about the changing molecular system, including the nature of the orbital from which ionization occurs and the geometry and orientation of the molecule. For extracting maximum information from PADs it is, however, necessary that the measurements are performed with respect to the molecular frame.

If the pump pulse leads to rapid dissociation, time-resolved molecular-frame photoelectron angular distributions (MFPADs) can be obtained by measuring the emission direction of the photoelectrons, produced by the probe pulse, in coincidence with a recoiling ionic fragment [4–6]. For the general case where the molecular orientation cannot be deduced from the recoil directions of the photo-fragments [7,8], or if dissociation does not occur at all [9,10], measurement of MFPADs require that the molecular orientation is fixed during the pump and the probe event. Moderately intense laser pulses can align [11] and, in combination with static electric fields, also orient [12] molecules, and as such provide the desired targets for measurements of time-resolved MFPADs [13,14]. The first demonstration of this approach was reported in 2009 for

photodissociation of CS<sub>2</sub> probed by single-photon ionization [15]. The fact that most molecules are nonlinear makes it an important goal to extend the method to the general class of asymmetric top molecules such that time-resolved MFPADs can be fully exploited for exploring ultrafast molecular dynamics.

Here we reach this goal for the case of the rotational dynamics of an asymmetric top molecule, naphthalene (C<sub>10</sub>H<sub>8</sub>), prealigned in the laboratory frame by a nanosecond (ns) laser pulse. In particular, rotation of the molecular plane around the long molecular axis (see Fig. 1) is initiated by a fs kick pulse and the time-dependent PADs, produced by strong-field ionization with a circularly polarized fs probe pulse, are measured. We report results both when the ns pulse aligns only the long axis of naphthalene,

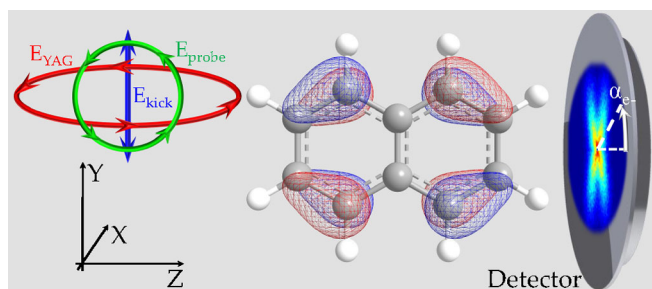


FIG. 1 (color online). Schematic of the key elements in the experiment. The polarization states of the three laser pulses are shown for the case when the naphthalene molecules are 3D aligned by the elliptically polarized YAG pulse (long molecular axis along the Z axis and short molecular axis along the Y axis) and electrons are detected (circularly polarized probe pulse). An isocontour surface (value 0.02) representation of the HOMO of naphthalene is overlaid on the molecular structure.

i.e., initial 1D alignment, and when the ns pulse aligns all three principal axes of naphthalene, i.e., initial 3D alignment. In the latter case, the degree of 3D alignment sharpens in a  $\sim 2$  ps interval just after the end of the kick pulse. As a result, the contrast of the observed structures in the MFPADs in this interval improves significantly. In particular, suppression of electron emission in nodal planes of the valence orbitals becomes much more pronounced in agreement with theory.

Most aspects of the experimental setup have been described before [12] and only a few important details will be pointed out (see Fig. 1). A pulsed molecular beam is formed by expanding 5 mbar naphthalene in 90 bar of He into vacuum. The molecules travel into a velocity map imaging spectrometer where they are crossed by three pulsed laser beams. The first pulse (YAG pulse:  $\lambda = 1064$  nm,  $\tau_{\text{FWHM}} = 10$  ns) serves to adiabatically align the molecules. The second pulse (kick pulse: 800 nm, 200 fs) initiates rotation around their long axis. The third pulse (probe pulse: 800 nm, 30 fs) is either linearly or circularly polarized. When linear, it is used to characterize the alignment of the molecular plane by Coulomb exploding the molecules and recording the recoiling  $\text{H}^+$  fragments. When circular, and at much lower intensity, it is used to singly ionize the molecules for the PAD measurements. The 2D  $\text{H}^+$  ion and electron images are recorded at different times  $t$  after the center of the kick pulse.

In Fig. 2 the YAG polarization is along the Z axis (perpendicular to the detector plane; see Fig. 1) and, therefore, the long axis (smallest moment of inertia axis), which is the most polarizable, will be confined along the Z axis. The circularly symmetric  $\text{H}^+$  ion image [Figure 2(a1)] obtained with only the YAG pulse and the probe pulse,

linearly polarized along the Z axis, shows that the orientation of the molecular plane around the fixed long axis is random as expected. When the kick pulse is applied, linearly polarized along the Y axis, the  $\text{H}^+$  ions gradually localize along the Y axis. The localization reaches a maximum around  $t = 1.00$  ps quantified by a maximum  $\langle \cos^2 \alpha_{\text{ion}} \rangle = 0.62$ , where  $\alpha_{\text{ion}}$  is the angle between the projection of the  $\text{H}^+$  ion velocity vector on the detector plane and the kick pulse polarization vector (along the Y direction). At this time the naphthalene molecules are 3D aligned with their long axis confined along the Z axis and the short axis confined along the Y axis. At later times the angular localization of the  $\text{H}^+$  ions gradually disappears due to dephasing of the rotational states excited by the kick pulse [16,17], although a weak confinement along the X axis occurs at  $t = 3.33$  ps. This antialignment corresponds to mild 3D alignment with the short axis along the X axis. The observations based on the  $\text{H}^+$  images are fully consistent with recent studies on 3,5 difluoriodobenzene [16,17].

Turning to the electron images shown in row (b) of Fig. 2, we first note that they are recorded at a reduced intensity of the probe pulse ( $8.0 \times 10^{13}$  W/cm<sup>2</sup>) where naphthalene only undergoes single ionization with minor fragmentation [18]. Based on the measured mass spectrum we estimate that of all molecules ionized at least 85% are left in a stable state of the cation. Second, the probe pulse is circularly polarized (in the YZ plane) implying that no recollision, induced by the strong probe field, of the freed electron with its parent ion occurs. When the molecules are 1D aligned the electrons emerge in a stripe centered along the Y axis [Fig. 2(b1)]. The elongated momentum distribution can be understood by the fact that upon detachment, occurring at the peak of the probe pulse, the electron gains

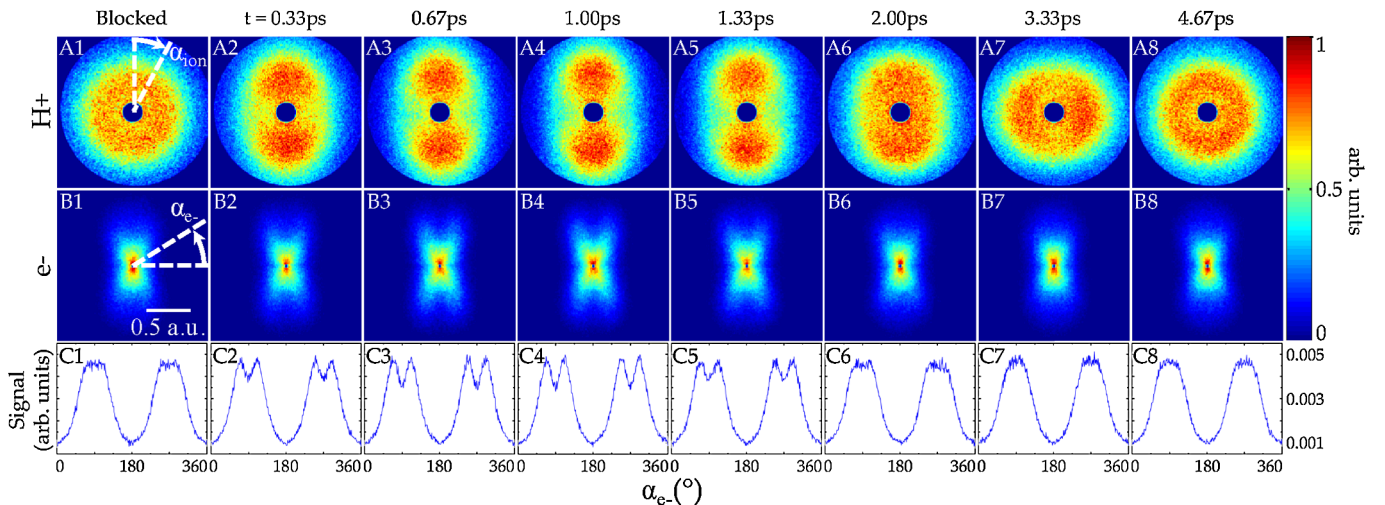


FIG. 2 (color online). Momentum images of  $\text{H}^+$  ions [row (a)] and electrons [row (b)] at different times after the kick pulse when 1D aligned naphthalene molecules are Coulomb exploded [row (a), linearly polarized probe pulse] or singly ionized [row (b), circularly polarized probe pulse]. Row (c) shows the corresponding PADs in the detector plane obtained by radially integrating the respective images from momentum 0.02 to 0.76 a.u. For the electron images the momentum scale is defined by the white bar (atomic units).  $I_{\text{probe}} = 3.2 \times 10^{14}$  W/cm<sup>2</sup> [ $8.0 \times 10^{13}$  W/cm<sup>2</sup>] in row (a) [rows (b) and (c)]. The YAG pulse is linearly polarized perpendicular to the detector plane (see Fig. 1) with  $I_{\text{YAG}} = 6 \times 10^{11}$  W/cm<sup>2</sup>.  $I_{\text{kick}} = 1.1 \times 10^{13}$  W/cm<sup>2</sup>.

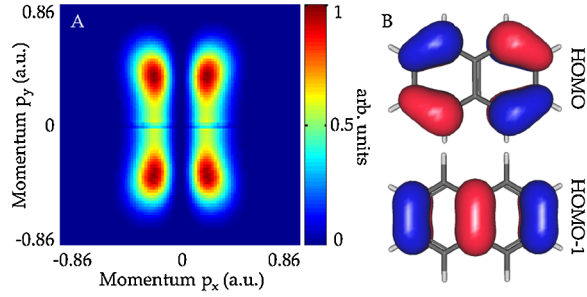


FIG. 3 (color online). (a) Calculated 2D electron momentum distribution for ionization of naphthalene, 3D aligned as shown on Fig. 1. The 30 fs circularly polarized probe pulse has a peak intensity  $8.0 \times 10^{13}$  W/cm<sup>2</sup> and volume averaging is included. (b) Contour plots of HOMO and HOMO-1.

momentum, in the polarization plane, from the remainder of the strong probe field [10,19]. At times after the kick pulse a pronounced structure develops in the electron images. Notably, the electron emission becomes suppressed along the  $Y$  axis seen as dips in the corresponding angular distributions [Figs. 2(c2)–2(c5)] at  $\alpha_{e-} = 90^\circ$  and  $270^\circ$ , where  $\alpha_{e-}$  is the angle measured counterclockwise with respect to the  $X$  direction [see Fig. 2(b1)]. The suppression is largest when the molecular plane is most tightly aligned along the  $(Y, Z)$  plane ( $t = 1.00$  ps). At this time the nodal plane of the highest-occupied molecular orbital (HOMO) [and the first orbital below HOMO in energy, HOMO-1; see Fig. 3(b)] that coincides with the molecular plane is aligned along the polarization plane of the probe pulse. As shown recently for a similar planar aromatic molecule, benzonitrile, this leads to suppressed electron emission in the polarization plane

and will manifest itself as the observed dips along the  $Y$  axis [10].

For the present case of naphthalene we calculated the MFPAD from single ionization with a circularly polarized pulse using the strong-field approximation corrected such that the induced Stark shifts of the neutral molecule and its cation ion are taken into account [20]. To model ionization from the HOMO we employed an  $f_{xyz}$  orbital. The results, displayed in Fig. 3(a), agree qualitatively with the experimental findings in Figs. 2(b3) and 2(b4). Quantitatively, the calculation predicts complete suppression of electron emission in the polarization plane of the probe pulse whereas the experimental PAD signal at  $\alpha_{e-} = 90^\circ$  and  $270^\circ$  only dips  $\sim 28\%$  with respect to the peak value. As shown below, stronger alignment of the molecular plane leads to much more pronounced dips in the PADs. Note that the presence of minima at  $0^\circ$  and  $180^\circ$  in both Figs. 2(c) and 4(c) is independent of the 3D alignment and reflects that electron emission is suppressed perpendicular to the polarization plane [21,22]

At longer times, where the confinement of the molecular plane is gradually lost, the pronounced dip in the PAD disappears because the nodal planes in the HOMO or HOMO-1 no longer coincide with the probe pulse polarization plane. At the time of the antialignment ( $t = 3.33$  ps) this will happen again for the nodal plane in the HOMO perpendicular to the molecular plane (and still containing the long axis; see Fig. 1). No suppression of electron emission along the  $Y$  axis is, however, observed—most likely because the planar confinement is too mild at the antialignment. Furthermore, ionization from HOMO-1 (ionization potential is 8.84 eV compared to 8.03 for the HOMO) may contribute because its nodal planes

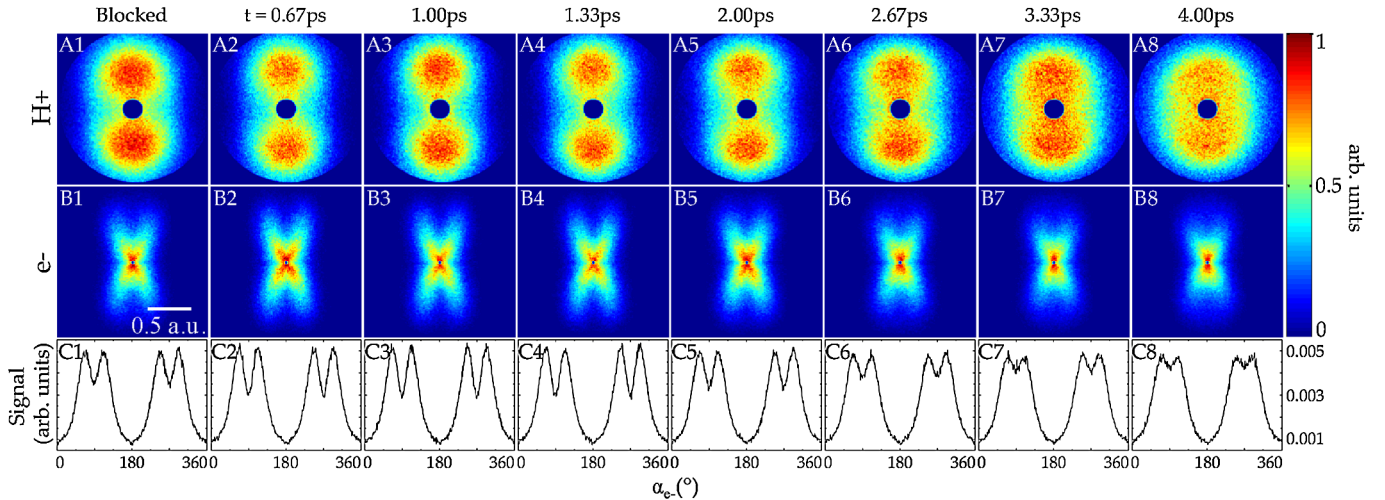


FIG. 4 (color online). Momentum images of  $H^+$  ions [row (a)] and electrons [row (b)] at different times after the kick pulse when 3D aligned naphthalene molecules are Coulomb exploded [row (a)] or singly ionized [row (b)]. Row (c) shows the corresponding PADs in the detector plane. For the electron images the momentum scale is defined by the white bar (atomic units). The probe pulse is linearly (circularly) polarized with an intensity of  $3.2 \times 10^{14}$  W/cm<sup>2</sup> [ $8.0 \times 10^{13}$  W/cm<sup>2</sup>] in row (a) [rows (b) and (c)]. The YAG pulse is elliptically polarized with the major axis perpendicular to the detector plane and an intensity ratio of 3:1.  $I_{YAG} = 6 \times 10^{11}$  W/cm<sup>2</sup> and  $I_{kick} = 5.5 \times 10^{12}$  W/cm<sup>2</sup>.



[Fig. 3(b)] do not coincide with the polarization plane when the molecule is antialigned.

Having shown that it is possible to measure the time-resolved PADs from strong-field ionization of naphthalene molecules, as they rotate around the fixed long axis, we proceed to study the case where naphthalene is 3D aligned prior to the kick pulse. This is accomplished by using an elliptically polarized YAG pulse with an intensity ratio between the major (along the  $Z$  axis) and the minor axis (along the  $Y$  axis) of 3:1. The  $H^+$  image [Fig. 4(a1)], recorded with the YAG pulse only, confirms the alignment of the molecular plane along the  $Y$  axis. From  $t = 0.33$  ps to  $t = 2.33$  ps  $\langle \cos^2 \alpha_{ion} \rangle$  falls in the range 0.64–0.68, which is higher than the value with the YAG pulse alone (0.63); i.e., the molecular plane is better aligned. This is similar to enhanced 1D alignment by the combination of a long and a short laser pulse reported previously [23,24]. The effect on the electron images is striking: The suppression of the electron emission along the  $Y$  axis is much more pronounced than with the elliptically polarized YAG alone. The dips in the PADs at  $\alpha_{e-} = 90^\circ$  and  $270^\circ$  go down to 46% of the peak value. With the elliptically polarized YAG pulse alone this number is 29%, almost the same as the most pronounced suppression obtained with the linearly polarized YAG pulse (at  $t = 1.00$  ps).

For  $t > 2$  ps the localization in the  $H^+$  images starts to decrease and concurrently the suppression in the electron images vanishes. We interpret this as the angular momentum of the molecular plane, gained by the kick pulse, is so high that the molecular plane simply rotates out of the angular range where it was originally confined by the YAG pulse. Our interpretation is corroborated by measurements at twice the fluence of the kick pulse where the delocalization of the  $H^+$  ions is even more pronounced and suppression in the electron images is absent.

This work contains the first experimental demonstration of fs time-resolved PADs from asymmetric top molecules that are fixed in space prior to the molecular process of interest. Here we studied the rotational motion of the molecular plane of naphthalene, but the combination of time-resolved PADs and prealigned (or preoriented) molecules will also apply to fundamental molecular transformations including dissociation and isomerization [25] and to the much faster motion of charge migration [26,27]. We showed that the ability to improve the degree of planar alignment, by the combination of an elliptically polarized alignment pulse and a short kick pulse, offers strong improvement in the sensitivity to the presence of nodal planes in strong-field ionization with circularly polarized fs pulses. In particular, the enhanced planar alignment (and thus 3D alignment [28]) persists for about 2 ps, which is sufficiently long that time-resolved experiments of intramolecular processes will benefit—both for strong-field probing and for extreme ultraviolet or x-ray probing using high-harmonic or free-electron laser sources.

The work was supported by the Lundbeck Foundation, the Carlsberg Foundation, the Danish Council for

Independent Research, and the European Marie Curie Initial Training Network CA-ITN-214962-FASTQUAST.

\*Corresponding author.

henriks@chem.au.dk

†Corresponding author.

bojer@phys.au.dk

- [1] A. Stolow, A. E. Bragg, and D. M. Neumark, *Chem. Rev.* **104**, 1719 (2004).
- [2] A. Stolow and J. G. Underwood, *Adv. Chem. Phys.* **139**, 497 (2008).
- [3] K. Reid, *Annu. Rev. Phys. Chem.* **54**, 397 (2003).
- [4] J. A. Davies, R. E. Continetti, D. W. Chandler, and C. C. Hayden, *Phys. Rev. Lett.* **84**, 5983 (2000).
- [5] A. M. Rijs, M. H. M. Janssen, E. t. H. Chrysostom, and C. C. Hayden, *Phys. Rev. Lett.* **92**, 123002 (2004).
- [6] O. Gessner *et al.*, *Science* **311**, 219 (2006).
- [7] Th. Weber *et al.*, *J. Phys. B* **34**, 3669 (2001).
- [8] M. L. Lipciuc and M. H. M. Janssen, *Phys. Chem. Chem. Phys.* **8**, 3007 (2006).
- [9] V. Kumarappan *et al.*, *Phys. Rev. Lett.* **100**, 093006 (2008).
- [10] L. Holmegaard *et al.*, *Nature Phys.* **6**, 428 (2010).
- [11] H. Stapelfeldt and T. Seideman, *Rev. Mod. Phys.* **75**, 543 (2003).
- [12] F. Filsinger *et al.*, *J. Chem. Phys.* **131**, 064309 (2009).
- [13] Here, alignment refers to confinement of molecule-fixed axes along laboratory-fixed axes, and orientation refers to the molecular dipole moment pointing in a particular direction.
- [14] Alternatively, resonant photoabsorption from the pump pulse can create mild 1D alignment in excited states; see Y. Tang, Y.-I. Suzuki, T. Horio, and T. Suzuki, *Phys. Rev. Lett.* **104**, 073002 (2010).
- [15] C. Z. Bisgaard *et al.*, *Science* **323**, 1464 (2009).
- [16] S. S. Viftrup *et al.*, *Phys. Rev. Lett.* **99**, 143602 (2007).
- [17] S. S. Viftrup *et al.*, *Phys. Rev. A* **79**, 023404 (2009).
- [18] A. N. Markevitch *et al.*, *Phys. Rev. A* **68**, 011402 (2003).
- [19] P. B. Corkum, N. H. Burnett, and F. Brunel, *Phys. Rev. Lett.* **62**, 1259 (1989).
- [20] D. Dimitrovski, C. P. J. Martiny, and L. B. Madsen, *Phys. Rev. A* **82**, 053404 (2010).
- [21] T. K. Kjeldsen, L. B. Madsen, and J. P. Hansen, *Phys. Rev. A* **74**, 035402 (2006).
- [22] N. B. Delone and V. P. Krainov, *J. Opt. Soc. Am. B* **8**, 1207 (1991).
- [23] M. D. Poulsen *et al.*, *Phys. Rev. A* **73**, 033405 (2006).
- [24] S. Guerin, A. Rouzee, and E. Hertz, *Phys. Rev. A* **77**, 041404 (2008).
- [25] C. B. Madsen *et al.*, *Phys. Rev. Lett.* **102**, 073007 (2009).
- [26] S. Luennemann, A. I. Kuleff, and L. S. Cederbaum, *J. Chem. Phys.* **129**, 104305 (2008).
- [27] A. I. Kuleff, S. Luennemann, and L. S. Cederbaum, *J. Phys. Chem. A* **114**, 8676 (2010).
- [28] Related studies on a molecule where the most polarizable axis can be imaged independently show that the axial alignment remains strong at the time when the planar alignment peak; S. S. Viftrup, Ph.D. thesis, Aarhus University, 2007.